Cancer Biomarkers -1 (2023) 1–11 1
DOI 10.3233/CBM-230104
IOS Press

A clinical spectrum of resectable lung adenocarcinoma with micropapillary component (MPC) concurrently presenting as mixed ground-glass opacity nodules

Ziwen Zhu[a], Weizhen Jiang[a], Danhong Zhou[a], Weidong Zhu[b,*] and Cheng Chen[a,*]
[a]*Department of Respiratory and Critical Medicine, The First Affiliated Hospital of Soochow University, Suzhou, Jiangsu, China*
[b]*Pathology Department, The First Affiliated Hospital of Soochow University, Suzhou, Jiangsu, China*

Received 19 March 2023
Accepted 10 October 2023

Abstract.
BACKGROUND: In clinical practice, preoperative identification of mixed ground-glass opacity (mGGO) nodules with micropapillary component (MPC) to facilitate the implementation of individualized therapeutic strategies and avoid unnecessary surgery is increasingly important
OBJECTIVE: This study aimed to build a predictive model based on clinical and radiological variables for the early identification of MPC in lung adenocarcinoma presenting as mGGO nodules.
METHODS: The enrolled 741 lung adenocarcinoma patients were randomly divided into a training cohort and a validation cohort (3:1 ratio). The pathological specimens and preoperative images of malignant mGGO nodules from the study subjects were retrospectively reviewed. Furthermore, in the training cohort, selected clinical and radiological variables were utilized to construct a predictive model for MPC prediction.
RESULTS: The MPC was found in 228 (43.3%) patients in the training cohort and 72 (41.1%) patients in the validation cohort. Based on the predictive nomogram, the air bronchogram was defined as the most dominant independent risk factor for MPC of mGGO nodules, followed by the maximum computed tomography (CT) value ($>$ 200), adjacent to pleura, gender (male), and vacuolar sign. The nomogram demonstrated good discriminative ability with a C-index of 0.783 (95%[CI] 0.744–0.822) in the training cohort and a C-index of 0.799 (95%[CI] 0.732–0.866) in the validation cohort Additionally, by using the bootstrapping method, this predictive model calculated a corrected AUC of 0.774 (95% CI: 0.770–0.779) in the training cohort.
CONCLUSIONS: This study proposed a predictive model for preoperative identification of MPC in known lung adenocarcinomas presenting as mGGO nodules to facilitate individualized therapy. This nomogram model needs to be further externally validated by subsequent multicenter studies.

Keywords: Mixed ground-glass opacity (mGGO), micropapillary component (MPC), lung adenocarcinoma, predictive model, nomogram

1. Introduction

The mixed ground-glass opacity (mGGO) nodule is a common imaging manifestation of early-stage lung adenocarcinoma [1]. In clinical practice, assessing the degree of malignancy mGGO nodules during imaging follow-up and finding the appropriate time for oper-

*Corresponding authors: Cheng Chen, Department of Respiratory and Critical Medicine, The First Affiliated Hospital of Soochow University, 899 Pinghai Road, Suzhou, Jiangsu 215006, China. Tel.: +86 13771775292; E-mail: chencheng@suda.edu.cn. Weidong Zhu, Pathology Department, The First Affiliated Hospital of Soochow University, 188 Shizi Street, Suzhou, Jiangsu 215006, China. E-mail: 16586088@qq.com.

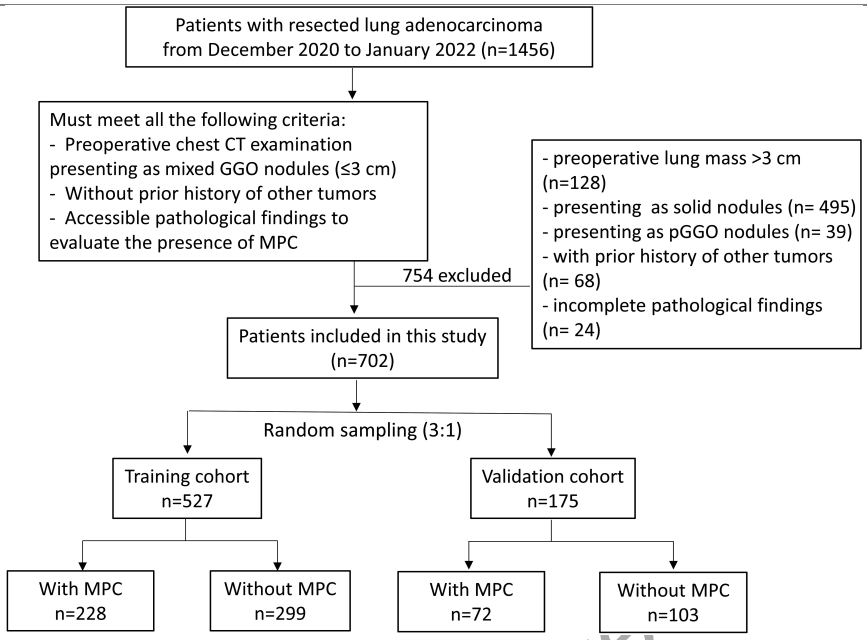

Fig. 1. Inclusion criteria and screening process of the study. The flow chart showed the process of patient enrollment, including the inclusion criteria and the grouping of study subjects.

ative intervention remain a clinical challenge [2–4]. Some studies observed that lung adenocarcinoma with the micropapillary component (MPC) also showed distinct genomic profiles and immunosuppression [5,6]. Additionally, numerous studies find that such patients also have a higher risk of early metastasis and exhibit a poorer prognosis even when the MPC component is not predominant [7–9]. Therefore, the early identification of mGGO nodule with MPC may help better judge the tumor characteristics in lung adenocarcinoma patients, which in turn can facilitate the implementation of individualized therapeutic strategies [10–12].

Given the diagnosis of MPC in adenocarcinoma requires pathological findings following surgical excision, effective preoperative predictive methods for the presence of MPC in GGO nodules are increasingly needed. Computed tomography (CT) is a non-invasive screening tool for lung cancer manifesting as GGO nodules and is widely used in clinical practice [13]. It was noticed that the internal radiological characteristics of solid-prominent nodules are often obscured and difficult to accurately evaluate [14] and the accuracy of pathological results between solid-predominant and mGGO nodules is also heterogeneous [15]. Therefore, the imaging prediction model established without distinguishing the purely solid nodules and mGGO nodules may reduce the predictive accuracy to a certain extent. Many studies have used imaging features of lung nodules, which include the solid-predominant nodules, to predict pathological subtypes of lung adenocarcinoma [16,17], but little to no research has focused on the mGGO nodules solely.

In this study, we aimed to retrospectively investigate the clinical and pathological features of mGGO nodules with MPC in lung adenocarcinoma patients. Furthermore, this study also constructed a nomogram to effectively predict the probability of MPC in mGGO by a non-invasive method.

2. Materials and methods

2.1. Patients and study design

This retrospective study was approved by the Institutional Review Boards of The First Affiliated Hospital of Soochow University (No.476 in 2022). Patients who underwent resection for lung adenocarcinoma from January 2021 to January 2022 were enrolled in this study. The flow chart of the study subjects is depicted in Fig. 1. The patients must meet all the following inclusion criteria: i, preoperative chest CT examination presenting as mGGO nodules ($\leqslant$ 3 cm); ii, without prior history of other tumors; iii, accessible pathological findings to evaluate the presence or absence of MPC.

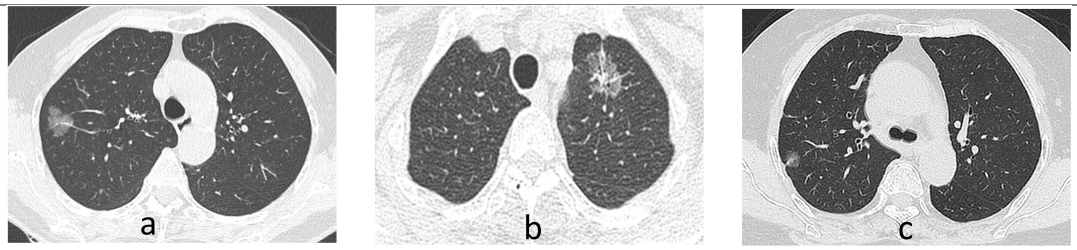

Fig. 2. Representative CT images of the study subjects. (a) A mixed ground ground-glass opacity (mGGO) nodule with homogeneous density in the right upper lobe Few blood vessels are penetrating within the mGGO and the margins appear lobulated; (b) A mGGO nodule in the upper left lobe that depicts vacuolar sign, vessel convergence, and pleural retraction; (c) A mGGO nodule adjacent to the pleura in the right upper lobe with pleural retraction.

Based on the presence or absence of the MPC in pathological findings, the training cohort and the validation cohort were divided into two groups respectively, the MPC group and the non-MPC group. The clinical and pathological data between the two groups in both cohorts were compared respectively. Accordingly, based on the univariate analysis, significant variables were selectly included in the multivariate analysis. Furthermore, a nomogram was constructed by selecting significant variables from the multivariate logistic analysis. And the discriminative and consistent ability of the predictive model was also validated.

2.2. Imaging assessment and pathological evaluation

We have reviewed the preoperative CT imaging of all enrolled subjects and some of the representative imaging findings are shown in Fig. 2. In particular, the imaging findings of mGGO nodules are standardly described, including the location of the lung lobes where the tumor is present and their relative position with pleura; the size of the tumor (maximum diameter); tumor margins (Lobulation, spiculation); internal features of the tumor (vacuolar sign, air bronchogram sigh, vessel convergence); adjacent to the pleura; and maximum CT values of the solid component.

The immunohistochemistry testing of programmed cell death-Ligand 1 (PD-L1) was conducted by 22C3 assays (Agilent Technologies) using the DakoAutostainer Link 48 platform following its manufacturer's instructions [18]. According to the tumor proportion score (TPS), cases were categorized into negative (TPS $<$ 1%), low expression (TPS: 1–50%) and high expression (TPS $>$ 50%). Additionally, Ki-67 in tumor tissue was quantified after employing immunohistochemistry of the tumor slide, and cases were further classified as negative (TPS $<$ 1%), low expression (TPS: 1–30%), and high expression (TPS $>$ 50%).

2.3. Definition

Mixed ground-glass opacity (mGGO) is defined as an opacity with increased density and the $0 <$ consolidation tumor ratio (CTR) $\leqslant 0.5$ [15,19]. The CT value is a relative value obtained by converting the detector's X-ray attenuation coefficient into a certain mathematical pattern. The micropapillary component (MPC) was confirmed based on the World Health Organization (WHO) criteria: a papillary cluster of tumor cells lacking a fibrovascular axis, and the micropapillary structure can be separated and/or linked to the alveolar wall [4,20]. Adjacent to the pleura was defined if there was no fat space between the tumor and the pleura or if the tumor directly extended into the pleura [21]. The pleural invasion was diagnosed when the elastic fiber staining showed that there was elastic fiber breakage in the visceral pleural elastic layer.

2.4. Statistical analysis

The random grouping method was conducted using R language and the enrolled 702 study subjects were randomly divided into two groups in a 3:1 ratio: the training cohort ($n = 527$) and the validation cohort ($n = 175$). Statistical analyses were conducted using SPSS software (version 25.0; IBM). Continuous variables regarding clinical and pathological characteristics between the micropapillary and non-micropapillary cohort were compared by Student's t-test or Mann-Whitney U-test, and categorical variables were compared by chi-square test or Fisher's exact test. Multivariate logistic regression was performed to identify imaging-based independent risk factors of the MPC in mGGO nodules. Especially, a 2-tailed p value < 0.05 was considered significant.

2.5. Nomogram construction and evaluation

As for the selection of relevant variables, the demographic information such as age, gender, and smoking

Table 1
Clinical and preoperative imaging characteristics between the enrolled subjects

Variates	MPC ($n = 300$)	Non-MPC ($n = 402$)	P value
Age (y)	63.0 (61.9–64.0)	59.9 (58.8–60.9)	**0.001**
Gender (male)	151 (50.3%)	131 (32.6%)	$<$ **0.001**
Smoking history	67 (22.3%)	63 (15.7%)	0.102
Location of lung lobe			0.374
Left upper lobe	69 (23.0%)	93 (23.1%)	
Left lower lobe	53 (17.7%)	49 (12.2%)	
Right upper lobe	75 (25.0%)	119 (29.6%)	
Right middle lobe	23 (7.7%)	35 (8.7%)	
Right lower lobe	37 (12.3%)	53 (13.2%)	
Multiple lung lobes	43 (14.3%)	53 (13.2%)	
Adjacent to pleura	211 (70.3%)	212 (52.7%)	$<$ **0.001**
Radiological features			
Lobulation	250 (83.3%)	306 (76.1%)	**0.020**
Spiculation	259 (86.3%)	307 (76.4%)	**0.001**
Vacuolar sign	206 (68.7%)	197 (49.0%)	$<$ **0.001**
Air bronchogram sigh	210 (70.0%)	143 (35.6%)	$<$ **0.001**
Vessel convergence	103 (34.3%)	132 (32.8%)	0.677
Maximum diameter (cm)			$<$ **0.001**
$\leqslant 2$	158 (52.7%)	291 (72.4%)	
> 2	142 (47.3%)	111 (27.6%)	
Maximum CT value			$<$ **0.001**
$\leqslant 200$	61 (20.3%)	194 (48.3%)	
> 200	239 (79.7%)	208 (51.7%)	

history were selected as variables based on previous literature. Variables regarding the internal and external characteristics of mGGOs were selected based on not only the literature but also the clinical practice. Based on the independent risk factors from multivariate logistic regression in the training cohort, a nomogram was plotted and validated by using the R programming language and environment (http://www.r-project.org/). In the training and validation cohort, the area under the curve (AUC) was used to evaluate the discriminative ability and the calibration curve was used to assess the agreement between the predicted risks and the actual results. The internal validation was implemented using the bootstrapping method by setting the number of iterations to 1000.

3. Results

3.1. Demographic features

A total of 702 patients were enrolled in the study and the MPC was found in 300 (42.7%) patients. Among them, 204 patients had growth of ground glass nodules during follow-up time, and 144 patients underwent preoperative biopsy. The comparisons of demographic features between the MPC group and the non-MPC group are shown in Table 1. The median age of the MPC group was 63. 0 years, which was higher than that of the non-MPC group (59.9, $p = 0.001$) Additionally, the proportion of males was also higher in the MPC group (50.3% vs. 32.6%, $p < 0.001$). As for the smoking history, there was no significant difference between the two groups (22.3% vs. 15.7%, $p = 0.102$). Additionally, the clinical characteristics of the training cohort and the validation cohort are shown as supplementary materials in Tables 4 and Table 5.

3.2. Imaging findings

The preoperative imaging characteristics between the MPC group and the non-MPC group are shown in Table 1. The location of the lung lobes for mGGO nodules was comparable between the MPC group and non-MPC group ($p > 0.05$). While mGGO nodules adjacent to the pleura were more likely to be found in the MPC group (70.3% vs. 52.7%, $p < 0.001$). Furthermore, the mGGO nodule from the MPC group was more likely to present a larger diameter (> 2 cm) compared with their counterparts (47.3% vs. 27.6%, $p < 0.001$).

In terms of marginal features of mGGO nodules, mGGO nodules with MPC were more likely to manifest as lobulation (83.3% vs. 76.1%, $p = 0.020$) and spiculation (86.3% vs. 76.4%, $p = 0.001$) than the non-MPC group. We then compared the internal characteristics of mGGO nodules between the two groups. The data suggested that mGGO with MPC was more likely to exhibit the vacuolar sign (68.7% vs. 49.0%, $p < 0.001$) and

Table 2
Multivariate analysis of risk factors for differentiating mGGO nodules with and without MPC in the training cohort

Variates	Univariate analysis			Multivariate analysis		
	P value	OR	95%CI	*P* value	Adjusted OR	95%CI
Age	0.002	1.03	1.01–1.05			
Gender (male)	< 0.001	2.12	1.48–3.02	0.006	1.78	1.18–2.68
Adjacent to pleura	< 0.001	2.09	1.45–3.02	< 0.001	2.37	1.56–3.61
Lobulation	0.047	1.56	1.00–2.41			
Spiculation	0.037	1.64	1.03–26.61			
Vacuolar sign	< 0.001	2.30	1.60–3.31	0.003	1.88	1.25–2.85
Air bronchogram	< 0.001	3.75	2.61–5.41	< 0.001	3.73	2.47–5.65
Maximum diameter (> 2 cm)	< 0.001	2.21	1.55–3.16			
Maximum CT value (> 200)	< 0.001	3.68	2.47–5.49	< 0.001	3.12	2.00–4.83

air bronchogram sign (70.0% vs. 35.6%, $p < 0.001$). However, the proportion of vessel convergence sign in mGGO nodules was comparable between the two groups (34.3% vs. 32.8%, $p = 0.677$). And it was noticed that the proportion of mGGO with a maximum CT value > 200 in the MPC group was significantly higher than that in the non-MPC group (79.7% vs. 51.7%, $p < 0.001$).

3.3. Independent risk factors for the presence of MPCin mGGO nodules in the training cohort

Firstly, we screened variables with statistical significance from the univariate analysis, including age, gender, adjacent to pleura, lobulation, spiculation, vacuolar sign, air bronchogram, maximum diameter (> 2 cm), and maximum CT value (> 200). According to the multivariate logistic regression analysis in the training cohort (Table 2), gender (male) (OR 1.78, 95%[CI] 1.18–2.68, $p = 0.006$), adjacent to pleura (OR 2.37, 95%[CI] 1.56–3.61, $p < 0.001$), vacuolar sign (OR 1.88, 95%[CI] 1.25–2.85, $p = 0.003$), air bronchogram sigh (OR 3.73 95%[CI] 2.47–5.65, $p < 0.001$), and the CT value (> 200) (OR 3.12, 95%[CI] 2.00–4.83, $p < 0.001$) were the independent risk factors for the presence of MPC in lung adenocarcinoma presenting as mGGO nodules.

3.4. The preoperative predictive nomogram construction and validation

As shown in Fig. 3a, based on the five significant variables from multivariate analysis in the training cohort, we constructed a nomogram for the prediction of MPC in lung adenocarcinoma patients presenting as mGGO nodules. Based on the predictive nomogram, the air bronchogram was defined as the most dominant independent risk factor for the presence of MPC in mGGO nodules, followed by the maximum CT value (> 200), adjacent to pleura, gender (male) and vacuolar sign.

Then the discriminative and consistent ability of the nomogram in the training cohort was validated. As shown in Fig. 3b, the cut-off score of the receiver operating characteristic (ROC) curve was 241.4 points and lung adenocarcinoma presenting as mGGO nodules could be further identified as MPC or non-MPC with a sensitivity of 72.4% and a specificity of 71.3%. Based on the ROC curve, favorable discrimination of the predictive ability was shown with an AUC value of 0.783 (95%[CI] 0.744–0.822), which demonstrated the satisfactory discrimination of the model. As for the consistent validation, in the training cohort, the calibration curve of the nomogram also showed high consistencies between the predicted and observed micropapillary-contained probability. Furthermore, the internal validation was implemented using the bootstrapping method by setting the number of iterations to 1000. And this predictive model calculated a corrected AUC of 0.774 (95% CI: 0.770–0.779).

3.5. The predictive nomogram validation in the validation cohort

Accordingly, we validated the predictive nomogram in the validation cohort (Fig. 4a and b). The predictive model also demonstrated favorable discriminative ability with an AUC value of 0.799 (95%[CI] 0.732–0.866) in the validation cohort. The calibration curve also showed consistencies between the predicted and observed micropapillary-contained probability.

3.6. mGGO nodules with MPC presented a higher aggressive potential

To assess the invasive potential of mGGO nodules with MPC, pleural and lymph node metastasis rates were compared between the two groups (Table 3). A

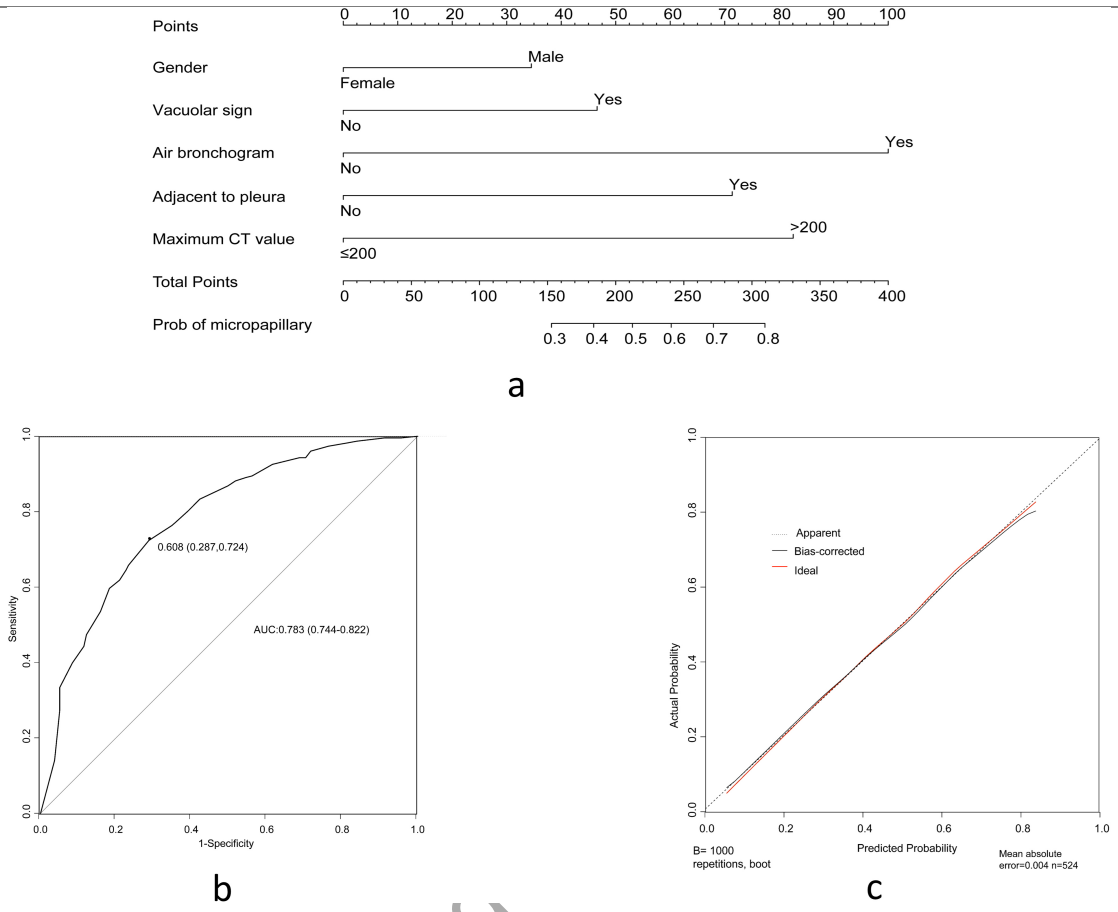

Fig. 3. The construction and validation of a predictive nomogram based on clinical and radiological features in the training cohort. (a) The nomogram for the prediction of MPC among lung adenocarcinoma presenting as mGGO nodules. Five categorical variables from the multivariate logistic analysis were included in the model and had different contributions to the probability of MPC among mGGO nodules; (b) A ROC curve for the discriminative validation of the nomogram in the training cohort. The AUC value of the ROC curve was 0.783 (95%[CI] 0.744–0.822); (c) A calibration curve for the estimation of agreement between the predicted mGGO nodules with MPC and those of the nomogram.

total of 60.4% (424/702) mGGO nodules adjacent to the pleura underwent pleural elastic fiber staining, including 207 cases in the MPC group and 217 cases in the non-MPC group. Typically, mGGO nodules adjacent to the pleura in the MPC group were more likely to occur pleural invasion compared to the non-MPC group (29.3% vs. 5.5%, $p < 0.001$).

Then we compared the lymph node metastasis rates between the MPC group and the non-MPC group. The lymph node biopsy was implemented in 135 cases from the MPC group and 117 cases from the non-MPC group. In particular, the pathological findings suggested a higher ratio of lymph node metastasis in the MPC group (18.5% vs. 0.9%, $p < 0.001$). The above finding suggested that the mGGO nodules with MPC presented a higher risk of pleural and lymph node invasion.

Notably, cases that tested with high Ki-67 expression ($> 30\%$) were more likely to be found in the MPC group than the non-MPC group (14.7% vs. 0.5%, $p < 0.001$). This indicated that mGGO nodules with MPC might have higher chances of metastasis and tumor proliferation potential.

3.7. *mGGO nodules with MPC were more likely to exhibit inhibitive tumor immune microenvironment*

To explore the immune microenvironment characteristics among lung adenocarcinoma patients with and without MPC, we then compared the expression of the immune inhibitory molecule PD-L1. According to the immunohistochemistry staining results (Table 3), the proportion of cases that tested positive for PD-L1 was significantly higher in the MPC group compared with their non-MPC counterparts (57.7% vs. 30.8%, $p <$

Table 3
Histopathological characteristics of the study subjects

Variates	MPC ($n = 300$)	Non-MPC ($n = 402$)	P value
Pleural elastic fiber staining	207	217	
Non-pleural invasion	147 (71.0%)	205 (94.5%)	$<$ **0.001**
Pleural invasion	60 (29.0%)	12 (5.5%)	
Lymph node dissection	135	117	
Non-metastasis	110 (81.5%)	116 (99.1%)	$<$ **0.001**
Metastasis	25 (18.5%)	1 (0.9%)	
PD-L1 (22C3)			$<$ **0.001**
Negative ($<$ 1%)	127 (42.3%)	278 (69.2%)	
Low expression (1–50%)	156 (52.0%)	121 (30.1%)	
High expression ($>$ 5%)	17 (5.7%)	3 (0.7%)	
Ki-67			$<$ **0.001**
Negative ($<$ 1%)	7 (2.3%)	18 (4.5%)	
Low expression (1–30%)	249 (83.0%)	382 (95.0%)	
High expression ($>$ 30%)	44 (14.7%)	2 (0.5%)	

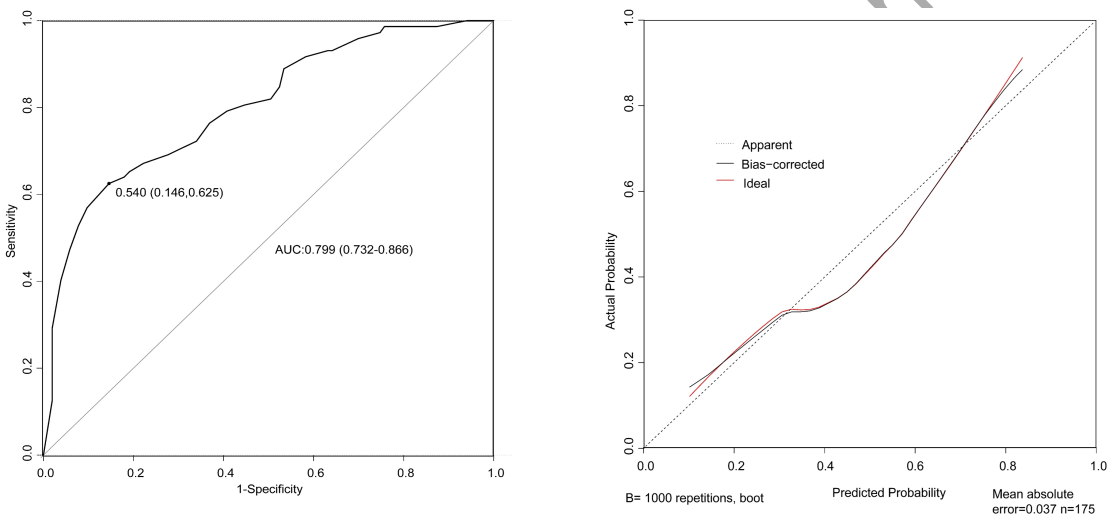

Fig. 4. The validation of the nomogram in the validation cohort. (a) A ROC curve for the discriminative validation of the nomogram from the training cohort. The AUC value of the ROC curve was 0.799 (95%[CI] 0.732–0.866) in the validation cohort; (b) A calibration curve for the estimation of agreement between the predicted mGGO nodules with MPC and those of the nomogram in the validation cohort.

0.001). The above data indicated that mGGO nodules with MPC were more likely to exhibit inhibitive tumor immune microenvironments.

4. Discussion

In this study, we found that the preoperative assessment of mGGO nodules with MPC implicated by clinical and radiological features could be very helpful for lung adenocarcinoma patients. Furthermore, we proposed an effective predictive nomogram to classify mGGO nodules with MPC in lung adenocarcinoma patients. It is a practical and non-invasive tool to assess the probability of MPC risk in mGGO nodules, thereby enabling timely identification for surgery and appropriate treatment when the samples are unobtainable.

Age and gender are controversial variables associated with pathological subtypes of lung adenocarcinoma [16,17,22]. In the present study, we found that the older ($>$ 65 y) and the male were mostly found in the non-MPC group. However, only gender was regarded as an indicator of MPC based on the multivariate analysis. As for the relationship between smoking history and the presence of MPC, in contrast with a study that indicated the proportion of smokers is associated with pathological subtypes of lung adenocarcinoma [8,23], the above finding was not shown in our data.

The current study supported previously reported findings that lung adenocarcinoma with MPC was more

Table 4
Clinical and preoperative imaging characteristics in the training and validation cohort

Variates	Training cohort			Validation cohort		
	MPC	Non-MPC	P value	MPC	Non-MPC	P value
No. of patients	228	299		72	103	
Age (y)	63.3 (62.1–64.5)	60.5 (59.3–61.7)	**0.002**	62.9 (60.7–64.0)	58.4 (55.7–61.1)	**0.036**
Gender (male)	114 (50%)	96 (32.1%)	$<$ **0.001**	37 (51.4%)	35 (34.0%)	**0.021**
Smoking history	52 (24.1%)	48 (15.1%)	0.749	15 (20.8%)	15 (14.6%)	0.279
Location of lung lobe			0.522			0.835
Left upper lobe	51 (22.4%)	69 (23.1%)		18 (25.0%)	24 (23.3%)	
Left lower lobe	44 (19.3%)	40 (13.4%)		9 (12.5%)	9 (8.7%)	
Right upper lobe	58 (25.4%)	85 (28.4%)		17 (23.6%)	34 (33.0%)	
Right middle lobe	15 (6.6%)	25 (8.4%)		8 (11.1%)	10 (9.7%)	
Right lower lobe	27 (11.8%)	40 (13.4%)		10 (13.9%)	13 (12.6%)	
Multiple lung lobes	33 (14.5%)	40 (13.3%)		10 (13.9%)	13 (12.6%)	
Adjacent to pleura	163 (71.5%)	163 (54.5%)	$<$ **0.001**	48 (66.7%)	49 (47.6%)	**0.012**
Radiological features						
Lobulation	190 (83.3%)	228 (76.3%)	**0.047**	60 (83.3%)	78 (75.7%)	0.225
Spiculation	196 (86.0%)	236 (78.9%)	**0.037**	63 (87.5%)	71 (68.9%)	**0.004**
Vacuolar sign	158 (69.3%)	148 (49.5%)	$<$ **0.001**	48 (66.7%)	49 (47.6%)	**0.002**
Air bronchogram sign	155 (68.0%)	108 (36.1%)	$<$ **0.001**	55 (74.6%)	35 (34.0%)	$<$ **0.001**
Vessel convergence	73 (32.0%)	101 (33.8%)	0.670	30 (41.7%)	31 (30.1%)	0.114
Maximum diameter (cm)			$<$ **0.001**			**0.001**
$\leqslant 2$	115 (50.4%)	207 (69.2%)		43 (59.7%)	84 (81.6%)	
> 2	113 (49.6%)	92 (30.8%)		29 (40.3%)	19 (18.4%)	
Maximum CT value			$<$ **0.001**			$<$ **0.001**
$\leqslant 200$	44 (19.3%)	140 (46.8%)		17 (23.6%)	54 (52.4%)	
> 200	184 (80.7%)	159 (53.2%)		55 (76.4%)	49 (47.6%)	

Table 5
Histopathological characteristics in the training and validation cohort

Variates	Training cohort			Validation cohort		
	MPC	Non-MPC	P value	MPC	Non-MPC	P value
No. of patients	228	299		72	103	
Pleural elastic fiber staining	152	160		55	57	
Non-pleural invasion	106 (69.7%)	149 (93.1%)	$<$ **0.001**	41 (74.5%)	56 (98.2%)	$<$ **0.001**
Pleural invasion	46 (30.3%)	11 (6.9%)		14 (25.5%)	1 (1.8%)	
Lymph node dissection	101	86		34	31	
Non-metastasis	83 (82.2%)	85 (98.8%)	$<$ **0.001**	27 (79.4%)	31 (100.0%)	**0.008**
Metastasis	18 (17.8%)	1 (1.2%)		7 (20.6%)	0 (0%)	
PD-L1 (22C3)			$<$ **0.001**			**0.009**
Negative ($<$ 1%)	94 (41.2%)	211 (70.6%)		33 (45.8%)	67 (65.0%)	
Low expression (1–50%)	120 (52.6%)	85 (28.4%)		36 (50.0%)	36 (35.0%)	
High expression ($>$ 5%)	14 (6.1%)	3 (1.0%)		3 (4.2%)	0 (0%)	
Ki-67			$<$ **0.001**			**0.003**
Negative ($<$ 1%)	7 (3.1%)	16 (5.4%)		0 (0%)	2 (1.9%)	
Low expression (1–30%)	184 (80.7%)	281 (94.0%)		65 (90.3%)	101 (98.1%)	
High expression ($>$ 30%)	37 (16.2%)	2 (0.7%)		7 (9.7%)	0 (0%)	

likely to be associated with lymphatic and pleural invasion [7,10]. Furthermore, for primary lung adenocarcinoma, a previous study demonstrated clinicopathological characteristics can provide predictive information of unexpected lymph node metastasis [23]. This further illustrated the importance of developing a pathological subtype predictive model, as this can also provide an early indication of the possibility of invasive capacity for primary lung adenocarcinoma.

The size was an important risk for the presence of MPC in lung adenocarcinoma according to previous research [15,24]. Our data showed that the proportion of mGGO nodules with a maximum diameter $>$ 2 cm was significantly higher in the MPC group, but it was not an independent risk factor for the presence of MPC. In addition, a previous study showed that the volume doubling time was an independent predictive factor for the pathological subtypes of lung adenocarcinoma, indicating that further investigation into the role of size doubling time in predicting the GGO nodules with MPC

may be needed [16].

Tumor spread through air spaces pattern has been reported as a novel invasive pattern in lung adenocarcinoma [25]. Notably, a study conducted by Yotsukura, M et al. showed that air bronchogram sign was significantly associated with tumor spread through air spaces pattern and vacuole was an independent predictor of this invasive pattern [26]. Interestingly, among the internal imaging features of mGGO nodules, our data also demonstrated that the vacuolar sign and air bronchogram sign were the independent risk factors for the presence of MPC in lung adenocarcinoma. The above information may indicate why the mGGO nodule with MPC has a higher invasion capability.

The CT value inside adenocarcinoma is diverse, reflecting cellularity, density, and heterogeneous histological components within the tumor [27]. Because the mGGO nodules with MPC were also more likely to be found with high invasive ability, the quantitative CT indicators are non-negligible predictive variables. A study demonstrated that among lung adenocarcinoma presenting as GGO nodules, the invasive components were more likely to appear in areas with high CT values while adherent components appear in the site with low CT values [28]. Similarly, a recent study by Koezuka et al. also found that the combined use of mean and maximum CT values was useful for predicting lepidic-predominant lung adenocarcinoma [29]. As expected, the maximum CT value was an important independent predictor for the MPC among mGGO nodules in this study.

This study has some limitations. Firstly, this is a single-center retrospective study and the results obtained need to be further validated by subsequent multicenter studies. Additionally, the study subjects included are more likely to have higher-risk nodules, which may lead to selection bias. Since our data were retrospectively derived from cases in recent years, the lack of longitudinal follow-up information in this study is another limitation that cannot be ignored. The data on genetic mutations in this study were not fully available and their correlation with lung adenocarcinoma with MPC also needs to be further explored. Finally, all the nodules included in this cohort were known adenocarcinoma, the predictive model proposed in this study cannot be used in a GGO nodule that has no tissue diagnosis.

5. Conclusion

The predictive nomogram based on the multivariate logistic regression analysis proposed in this study showed that the air bronchogram was the most dominant independent risk factor for the presence of MPC in known lung adenocarcinoma presenting as mGGOs, followed by the maximum CT value (> 200), adjacent to pleura, gender (male), and vacuolar sign. The predictive nomogram proposed in this study is a convenient tool for early prediction of MPC in lung adenocarcinoma presenting as mGGO nodules. With the help of this predictive model, individualized surgical and therapeutic strategies could be implemented for patients with lung adenocarcinoma diagnosed as mGGO nodules with suspected MPC. This nomogram model needs to be further externally validated by subsequent multicenter studies.

Abbreviations

mGGO: Mixed ground-glass opacity
MPC: Micropapillary component
AUC: Area under the curve
CT: Computed tomography
PD-L1: Programmed cell death-Ligand 1
ROC: Receiver operating characteristic

Acknowledgments

We would like to thank all the nurses and the clinical staff who provided care for the patient. We thank the funders of the National Natural Science Foundation of China (NSFC) grant (grant number 81672280), Jiangsu Provincial Medical Key Discipline (grant number ZDXK202201) and Project of Suzhou City (grant number SYS2021034) for supporting this work.

Author contributions

Conception: Cheng Chen and Weidong Zhu.
Interpretation or analysis of data: Ziwen Zhu and Weizhen Jiang.
Preparation of the manuscript: Danhong Zhou.
Revision for important intellectual content: Ziwen Zhu.
Supervision: Cheng Chen and Weidong Zhu.

Funding

The project was mainly supported by the National Natural Science Foundation of China (NSFC) grant (grant number 81672280), Jiangsu Provincial Medical Key Discipline (grant number ZDXK202201) and Project of Suzhou City (grant number SYS2021034).

Competing interests

The authors have no relevant financial or non-financial interests to disclose.

Ethics approval

This study was performed in line with the principles of the Declaration of Helsinki. This study was approved by the Institutional Review Boards of The First Affiliated Hospital of Soochow University (No.476 in 2022).

References

[1] H. Sung, J. Ferlay, R.L. Siegel, M. Laversanne, I. Soerjomataram, A. Jemal and F. Bray, Global Cancer Statistics 2020: GLOBOCAN Estimates of Incidence and Mortality Worldwide for 36 Cancers in 185 Countries, *CA Cancer J Clin* **71** (2021), 209–249.

[2] R. Qu, D. Tu, Y. Cai, W. Ping and X. Fu, Clinical features and surgical outcomes of young patients with lung adenocarcinoma manifesting as ground glass opacity, *Front Oncol* **12** (2022), 979522.

[3] Y. Zhang, Z. Chen, H. Hu and H. Chen, Surgical Strategies for Pre- and Minimally Invasive Lung Adenocarcinoma 3.0: Lessons Learned From the Optimal Timing of Surgical Intervention, *Semin Thorac Cardiovasc Surg* **34** (2022), 311–314.

[4] K.J. Butnor, Controversies and challenges in the histologic subtyping of lung adenocarcinoma, *Transl Lung Cancer Res* **9** (2020), 839–846.

[5] Y. Huo, L. Sun, J. Yuan, H. Zhang, Z. Zhang, L. Zhang, W. Huang, X. Sun, Z. Tang, Y. Feng, H. Mo, Z. Yang, C. Zhang, Z. Yu, D. Yue, B. Zhang and C. Wang, Comprehensive analyses unveil novel genomic and immunological characteristics of micropapillary pattern in lung adenocarcinoma, *Front Oncol* **12** (2022), 931209.

[6] V. Tancoš, M. Grendár, A. Farkašová, Z. Hutka, J. Mičák, Z. Kviatkovská, T.C. Hardman, G.A.D. Hardy and L. Plank, Programmed death ligand 1 protein expression, histological tumour differentiation and intratumoural heterogeneity in pulmonary adenocarcinoma, *Pathology* **52** (2020), 538–545.

[7] K. Wang, M. Xue, J. Qiu, L. Liu, Y. Wang, R. Li, C. Qu, W. Yue and H. Tian, Genomics Analysis and Nomogram Risk Prediction of Occult Lymph Node Metastasis in Non-Predominant Micropapillary Component of Lung Adenocarcinoma Measuring $\leqslant$ 3 cm, *Front Oncol* **12** (2022), 945997.

[8] P. Bertoglio, V. Aprile, L. Ventura, M. Cattoni, D. Nachira, F. Lococo, M.R. Perez, F. Guerrera, F. Minervini, G. Querzoli, G. Bocchialini, D. Bacchin, F. Franzi, G. Rindi, S. Bellafiore, F. Femia, G.S. Bogina, P. Solli, P. Kestenholz, E. Ruffini, M. Paci, S. Margaritora, A.S. Imperatori, M. Lucchi, L. Gnetti and A.C. Terzi, Impact of High-Grade Patterns in Early-Stage Lung Adenocarcinoma: A Multicentric Analysis, *Lung* **200** (2022), 649–660.

[9] B. Peng, G. Li and Y. Guo, Prognostic significance of micropapillary and solid patterns in stage IA lung adenocarcinoma, *Am J Transl Res* **13** (2021), 10562–10569.

[10] S.H. Choi, J.Y. Jeong, S.Y. Lee, K.M. Shin, S.Y. Jeong, T.I. Park, Y.W. Do, E.B. Lee, Y. Seok, W.K. Lee, J.E. Park, S. Park, Y.H. Lee, H. Seo, S.S. Yoo, J. Lee, S.I. Cha, C.H. Kim and J.Y. Park, Clinical implication of minimal presence of solid or micropapillary subtype in early-stage lung adenocarcinoma, *Thorac Cancer* **12** (2021), 235–244.

[11] Y. Hou, W. Song, M. Chen, J. Zhang, Q. Luo, S.W. Um, F. Facchinetti, S. Bongiolatti and Q. Zhou, The presence of lepidic and micropapillary/solid pathological patterns as minor components has prognostic value in patients with intermediate-grade invasive lung adenocarcinoma, *Transl Lung Cancer Res* **11** (2022), 64–74.

[12] P. Li, L. Liu, D. Wang, R. Yang, Y. Xuan, Y. Han, J. Wang, L. Guo, L. Zhang, S. Zhang and Y. Wang, Genomic and clinicopathological features of lung adenocarcinomas with micropapillary component, *Front Oncol* **12** (2022), 989349.

[13] B. Ouyang, M. Li, L. Li, S. Liu and M. Li, Characteristics of Ground-Glass Nodules Detected by Low-Dose Computed Tomography as a Regular Health Examination Among Chinese Hospital Employees and Their Parents, *Front Oncol* **11** (2021), 661067.

[14] D. Halpenny, K. Das, E. Ziv, A. Plodkowski, J. Zheng, M. Capanu, N. Rekhtman, J. Montecalvo, S.B. Solomon and M.S. Ginsberg, Percutaneous computed tomography guided biopsy of sub-solid pulmonary nodules: differentiating solid from ground glass components at the time of biopsy, *Clin Imaging* **69** (2021), 332–338.

[15] P.C. Tsai, Y.C. Yeh, P.K. Hsu, C.K. Chen, T.Y. Chou and Y.C. Wu, CT-Guided Core Biopsy for Peripheral Sub-solid Pulmonary Nodules to Predict Predominant Histological and Aggressive Subtypes of Lung Adenocarcinoma, *Ann Surg Oncol* **27** (2020), 4405–4412.

[16] S. Park, S.M. Lee, S. Kim, J.G. Lee, S. Choi, K.H. Do and J.B. Seo, Volume Doubling Times of Lung Adenocarcinomas: Correlation with Predominant Histologic Subtypes and Prognosis, *Radiology* **295** (2020), 703–712.

[17] Y. Xu, W. Ji, L. Hou, S. Lin, Y. Shi, C. Zhou, Y. Meng, W. Wang, X. Chen, M. Wang and H. Yang, Enhanced CT-Based Radiomics to Predict Micropapillary Pattern Within Lung Invasive Adenocarcinoma, *Front Oncol* **11** (2021), 704994.

[18] F. Fu, C. Deng, W. Sun, Q. Zheng, Y. Jin, Y. Li, Y. Zhang and H. Chen, Distribution and concordance of PD-L1 expression by routine 22C3 assays in East-Asian patients with non-small cell lung cancer, *Respir Res* **23** (2022), 302.

[19] Z.R. Liang, M. Ye, F.J. Lv, B.J. Fu, R.Y. Lin, W.J. Li and Z.G. Chu, Differential diagnosis of benign and malignant patchy ground-glass opacity by thin-section computed tomography, *BMC Cancer* **22** (2022), 1206.

[20] A. Marx, J.K. Chan, J.M. Coindre, F. Detterbeck, N. Girard, N.L. Harris, E.S. Jaffe, M.O. Kurrer, E.M. Marom, A.L. Moreira, K. Mukai, A. Orazi and P. Ströbel, The 2015 World Health Organization Classification of Tumors of the Thymus: Continuity and Changes, *J Thorac Oncol* **10** (2015), 1383–95.

[21] L. Miao, L. Yang, J.X. Zhang, X.J. Sun, H.H. Zhang, L.L. Qi and M. Li, Micronodular thymoma with lymphoid stroma: Contrast-enhanced CT features with histopathological correlation in 10 patients, *Front Oncol* **12** (2022), 964882.

[22] S. Park, S.M. Lee, H.N. Noh, H.J. Hwang, S. Kim, K.H. Do and J.B. Seo, Differentiation of predominant subtypes of lung adenocarcinoma using a quantitative radiomics approach on CT, *Eur Radiol* **30** (2020), 4883–4892.

[23] J.H. Hong, S. Park, H. Kim, J.M. Goo, I.K. Park, C.H. Kang, Y.T. Kim and S.H. Yoon, Volume and Mass Doubling Time of Lung Adenocarcinoma according to WHO Histologic Classification, *Korean J Radiol* **22** (2021), 464–475.

[24] M. Jia, S. Yu, L. Cao, P.L. Sun and H. Gao, Clinicopathologic

Features and Genetic Alterations in Adenocarcinoma In Situ and Minimally Invasive Adenocarcinoma of the Lung: Long-Term Follow-Up Study of 121 Asian Patients, *Ann Surg Oncol* **27** (2020), 3052–3063.

[25] K. Masai, H. Sakurai, A. Sukeda, S. Suzuki, K. Asakura, K. Nakagawa, H. Asamura, S.I. Watanabe, N. Motoi and N. Hiraoka, Prognostic Impact of Margin Distance and Tumor Spread Through Air Spaces in Limited Resection for Primary Lung Cancer, *J Thorac Oncol* **12** (2017), 1788–1797.

[26] L. Qin, Y. Sun, R. Zhu, B. Hu and J. Wu, Clinicopathological and CT features of tumor spread through air space in invasive lung adenocarcinoma, *Front Oncol* **12** (2022), 959113.

[27] D. Eriguchi, Y. Shimada, K. Imai, H. Furumoto, T. Okano, R. Masuno, J. Matsubayashi, N. Kajiwara, T. Ohira and N. Ikeda, Predictive accuracy of lepidic growth subtypes in early-stage adenocarcinoma of the lung by quantitative CT histogram and FDG-PET, *Lung Cancer* **125** (2018), 14–21.

[28] S. Koezuka, T. Mikami, N. Tochigi, A. Sano, Y. Azuma, T. Makino, H. Otsuka, K. Matsumoto, N. Shiraga and A. Iyoda, Toward improving prognosis prediction in patients undergoing small lung adenocarcinoma resection: Radiological and pathological assessment of diversity and intratumor heterogeneity, *Lung Cancer* **135** (2019), 40–46.

[29] S. Koezuka, A. Sano, Y. Azuma, T. Sakai, K. Matsumoto, N. Shiraga, T. Mikami, N. Tochigi, Y. Murakami and A. Iyoda, Combination of mean CT value and maximum CT value as a novel predictor of lepidic predominant lesions in small lung adenocarcinoma presenting as solid nodules, *Sci Rep* **12** (2022), 5450.